PHYSICAL REVIEW D **92,** 055010 (2015)

NLSP gluino and NLSP stop scenarios from $b-\tau$ Yukawa unification

Shabbar Raza,[1,2,*] Qaisar Shafi,[2,†] and Cem Salih Ün[2,3,‡]

[1]*State Key Laboratory of Theoretical Physics and Kavli Institute for Theoretical Physics China (KITPC), Institute of Theoretical Physics, Chinese Academy of Sciences, Beijing 100190, People's Republic of China*

[2]*Department of Physics and Astronomy, Bartol Research Institute, University of Delaware, Newark, Delaware 19716, USA*

[3]*Department of Physics, Uludağ University, Bursa TR16059, Turkey*

(Received 2 January 2015; published 9 September 2015)

We present a study of the $b-\tau$ Yukawa unified supersymmetric $SU(4)_c \times SU(2)_L \times SU(2)_R$ model (with $\mu > 0$), which predicts the existence of gluino—neutralino and stop—neutralino coannihilation scenarios compatible with the desired relic lightest supersymmetric particle neutralino dark matter abundance and other collider constraints. The next to lightest supersymmetric particle (NLSP) gluino or NLSP stop masses vary between 400 GeV and ∼1 TeV. The NLSP gluinos will be accessible at the 14 TeV LHC, while we hope that the NSLP stop solutions will be probed in future LHC searches. We also identify regions of the parameter space in which the gluino and the lighter stop are closely degenerate in mass, interchangeably playing the role of NLSP and next to next to lightest supersymmetric particle (NNLSP). We also update a previous study of $t-b-\tau$ Yukawa unification and show that NLSP gluino of mass ∼1 TeV, with a mass difference between the gluino and neutralino of less than 80 GeV, can be realized, consistent with the current collider and astrophysical constraints. We present benchmark points for $b-\tau$ and $t-b-\tau$ Yukawa unification that can be accessible at the LHC.

DOI: 10.1103/PhysRevD.92.055010 PACS numbers: 12.60.Jv, 12.60.-i, 14.80.Ly

I. INTRODUCTION

The discovery of the Higgs boson at the Large Hadron Collider (LHC) [1,2] is a big boost for the standard model (SM). Supersymmetry (SUSY) is arguably the prime candidate for beyond the SM physics and the minimal supersymmetric extension of the SM (MSSM) leads in a natural way to the gauge coupling unification and provides a solution to the gauge hierarchy problem. In addition, with the assumption of R-parity conservation, MSSM also provides a plausible candidate particle for dark matter, namely the lightest supersymmetric particle (LSP). Besides gauge coupling unification, models such as SUSY $SO(10)$ and SUSY $SU(4)_c \times SU(2)_L \times SU(2)_R$ $(4-2-2)$ also suggest $t-b-\tau$ Yukawa unification (YU) [3–9]. The $4-2-2$ structure allows us to consider nonuniversal gaugino masses with

$$M_1 = \frac{3}{5}M_2 + \frac{2}{5}M_3, \tag{1}$$

where M_1, M_2 and M_3 are the soft supersymmetry breaking (SSB) mass terms respectively for $U(1)_Y$, $SU(2)_L$ and $SU(3)_c$ gauginos. Equation (1) follows from the fact that the hypercharge generator of $U(1)_Y$ is derived as $Y = 3/5M_2 + 2/5M_3$, and the assumption of left-right symmetry at $M_{\rm GUT}$ which requires unification of the gauge couplings ($g_L = g_R$) and equality of the gauginos ($M_L = M_R \equiv M_2$) associated with the $SU(2)_L$ and $SU(2)_R$ gauge groups. Furthermore, if the $4-2-2$ symmetry breaks to the MSSM gauge group at around $M_{\rm GUT}$, the threshold corrections to the gauge couplings become negligible and unification of the MSSM gauge couplings is approximately maintained.

Supersymmteric $4-2-2$ offers a rich phenomenology, which can be examined in particular at the LHC. As far as we know, it is the only model which requires next to lightest supersymmetric particle (NLSP) gluino to bring the relic abundance of LSP neutralino within the observed range of dark matter density in the presence of $t-b-\tau$ YU [6,8]. It was also shown that $t-b-\tau$ YU in $4-2-2$ with the same sign SSB gaugino mass terms is compatible with neutralino dark matter through the gluino coannihilation channel [6,8,10,11]. Considering opposite sign gauginos with $\mu < 0, M_2 < 0$ and $M_3 > 0$ (where μ is the bilinear Higgs mixing term) in [9], $t-b-\tau$ YU consistent with known experimental constraints was achieved in $4-2-2$ for $m_{16} \gtrsim 300$ GeV, as opposed to $m_{16} \gtrsim 8$ TeV for the case of same sign gaugino masses. Here m_{16} denotes the common soft SUSY breaking scalar mass at M_{GUT}. Besides low m_{16} values, $4-2-2$ with relative sign gauginos predicts the existence of stau-neutralino coannihilation channel, bino-wino mixing and A-resonance solutions. However, in this case, there is no solution with NLSP stop or NLSP gluino, since their masses are predicted to be around ≳3–4 TeV [9].

Even though the $4-2-2$ framework allows $t-b-\tau$ YU, this unification, in general, does not have to hold when one considers higher dimensional operators. However, if a

*shabbar@itp.ac.cn
†shafi@bartol.udel.edu.
‡cemsalihun@uludag.edu.tr

set of higher dimensional operators is considered whose contributions to the Yukawa couplings are expressed as $y_e/y_d = 1$ and $y_u/y_d \neq 1$ [12], one can configure a setup for $4-2-2$ in which the $b-\tau$ YU is maintained, while $t-b-\tau$ YU does not hold. We show in this paper that relaxing $t-b-\tau$ YU to $b-\tau$ YU in the presence of some contributions to the Yukawa couplings such as those from the higher dimensional operators [12] yields NLSP stop solutions in addition to NLSP gluino. We also find that the NLSP stop is nearly degenerate with the LSP neutralino, and hence the decay $\tilde{t}_1 \to c\tilde{\chi}_1^0$ is the only channel kinematically allowed. The ATLAS collaboration has recently searched for such decays for the first time, and the results have excluded NLSP stop up to 270 GeV for LSP neutralino with mass of about 200 GeV [13]. The CMS collaboration has ruled out NLSP stop of mass $\lesssim 250$ GeV, if the mass difference with LSP neutralino is less than 10 GeV [14]. We obtain relatively heavy ($600 \lesssim m_{\tilde{t}_1} \lesssim 900$ GeV) NSLP stop solutions, and we hope that future searches will be able to test our results. We also identify some solutions for which the mass difference between the NLSP and next to next to lightest supersymmetric particle (NNLSP) is small. We find such solutions in both the NLSP stop and NLSP gluino scenarios.

We also devote a section to $t-b-\tau$ YU in $4-2-2$ to update the results and compare with $b-\tau$ YU. We analyze the data that we obtain in light of the current experimental constraints including the discovery of the Higgs boson of mass close to 125 GeV, flavor physics and WMAP9. The LHCb collaboration has recently discovered $B_s \to \mu^+\mu^-$ with the branching fraction $BF(B_s \to \mu^+\mu^-) = 3.2^{+1.5}_{-1.2} \times 10^{-9}$ [15] that is consistent with the SM prediction of $(3.2 \pm 0.2) \times 10^{-9}$ [16]. In MSSM, this flavor changing decay receives contributions from the exchange of the pseudoscalar Higgs boson A [17], which is proportional to $(\tan\beta)^6/m_A^4$. Since $t-b-\tau$ YU requires large $\tan\beta (\gtrsim 40)$, it is important to see the impact of $B_s \to \mu^+\mu^-$ discovery on $4-2-2$ parameter space in the presence of $t-b-\tau$ YU.

The fundamental parameters of the model include

$$m_{16}, M_2, M_3, A_0/m_{16}, m_{H_d}, m_{H_u}, \tan\beta, \qquad (2)$$

where m_{16} is the universal SSB mass term for sfermions, and M_2, M_3 are the SSB gaugino mass terms for $SU(2)_L$ and $SU(3)_c$ respectively. A_0 is the universal SSB trilinear interaction coupling, m_{H_d} and m_{H_u} are SSB mass terms respectively for the up and down type Higgs scalars of the MSSM and $\tan\beta$ is the ratio of the MSSM Higgs vacuum expectation values.

The outline for the rest of the paper is as follows. In Sec. II we summarize the scanning procedure and the experimental constraints applied in our analysis. We present our findings for $b-\tau$ and $t-b-\tau$ YU in Sec. III, and we also provide a table with five benchmark points that illustrate our results. Our conclusion is summarized in Sec. IV.

II. SCANNING PROCEDURE AND PHENOMENOLOGICAL CONSTRAINTS

We employ the ISAJET 7.84 package [18] to perform random scans over the parameter space given below. In this package, the weak scale values of gauge and third generation Yukawa couplings are evolved to $M_{\rm GUT}$ via the MSSM renormalization group equations (RGEs) in the $\overline{DR}$ regularization scheme. We do not strictly enforce the unification condition $g_3 = g_1 = g_2$ at $M_{\rm GUT}$, since a few percent deviation from unification can be assigned to unknown grand unified theory (GUT)-scale threshold corrections [19]. With the boundary conditions given at $M_{\rm GUT}$, all the SSB parameters, along with the gauge and Yukawa couplings, are evolved back to the weak scale $M_{\rm Z}$.

In evaluating Yukawa couplings the SUSY threshold corrections [20] are taken into account at the common scale $M_{\rm SUSY} = \sqrt{m_{\tilde{t}_L} m_{\tilde{t}_R}}$. The entire parameter set is iteratively run between $M_{\rm Z}$ and $M_{\rm GUT}$ using the full two-loop RGEs until a stable solution is obtained. To better account for leading-log corrections, one-loop step-beta functions are adopted for gauge and Yukawa couplings, and the SSB parameters m_i are extracted from RGEs at appropriate scales $m_i = m_i(m_i)$. The RGE-improved one-loop effective potential is minimized at an optimized scale $M_{\rm SUSY}$, which effectively accounts for the leading two-loop corrections. Full one-loop radiative corrections are incorporated for all sparticle masses.

The requirement of radiative electroweak symmetry breaking (REWSB) [21] puts an important theoretical constraint on the parameter space. Another important constraint comes from limits on the cosmological abundance of stable charged particles [22]. This excludes regions in the parameter space where charged SUSY particles, such as $\tilde{\tau}_1$ or $\tilde{t}_1$, become the LSP. We accept only those solutions for which one of the neutralinos is the LSP and saturates the dark matter relic abundance bound observed by WMAP9.

We have performed random scans for the following parameter range:

$$\begin{aligned}
0 &\le m_{16} \le 20 \text{ TeV} \\
0 &\le M_2 \le 5 \text{ TeV} \\
0 &\le M_3 \le 5 \text{ TeV} \\
-3 &\le A_0/m_{16} \le 3 \\
2 &\le \tan\beta \le 60 \\
0 &\le m_{H_u} \le 20 \text{ TeV} \\
0 &\le m_{H_d} \le 20 \text{ TeV}
\end{aligned} \qquad (3)$$

with $\mu > 0$ and $m_t = 173.3$ GeV [23]. Note that our results are not too sensitive to one or two sigma variation in the value of m_t [24]. We use $m_b^{\overline{DR}}(M_{\rm Z}) = 2.83$ GeV which is hard-coded into ISAJET.

In scanning the parameter space, we employ the Metropolis-Hastings algorithm as described in [25]. The data points collected all satisfy the requirement of REWSB, with the neutralino in each case being the LSP. After collecting the data, we impose the mass bounds on all the particles [22] and use the IsaTools package [26,27] and Ref. [28] to implement the phenomenological constraints from the Higgs boson [1,2], rare decays of B meson [15,29,30], and the dark matter observations [31] as follows:

$$m_h = 123 - 127\ \text{GeV} \tag{4}$$

$$0.8\times 10^{-9} \le \text{BR}(B_s \to \mu^+\mu^-) \le 6.2\times 10^{-9}(2\sigma) \tag{5}$$

$$2.99\times 10^{-4} \le \text{BR}(b \to s\gamma) \le 3.87\times 10^{-4}(2\sigma) \tag{6}$$

$$0.15 \le \frac{\text{BR}(B_u \to \tau\nu_\tau)_{\text{MSSM}}}{\text{BR}(B_u \to \tau\nu_\tau)_{\text{SM}}} \le 2.41(3\sigma) \tag{7}$$

$$0.0913 \le \Omega_{\text{CDM}}h^2(\text{WMAP9}) \le 0.1363(5\sigma) \tag{8}$$

An approximate error of about 2 GeV in calculating the Higgs boson mass arises from theoretical uncertainties in the calculation of the minimum of the scalar potential, and to a lesser extent from the experimental uncertainties in the values for m_t and α_s. Hence we allow solutions which predict the Higgs boson mass in an interval given in Eq. (4) rather than being strictly ∼125–126 GeV. The experimental measurements of the rare processes $B_s \to \mu^+\mu^-$ and $b \to s\gamma$ have a strong impact on the parameter space of supersymmetric models, and hence we allow solutions consistent with these constraints within 2σ deviation. On the other hand, the constraint from $B_u \to \tau\nu_\tau$ does not provide a stringent bound, and so we relax it to 3σ deviation.

Another stringent bound is provided by the WMAP bound on the relic abundance of neutralino LSP. Considering the uncertainties in the calculation of relic abundance of neutralino LSP, we allow our solutions to be consistent with the WMAP bound within 5σ. In this paper, the dark matter abundance is saturated only by the lightest neutralino. In this case, the WMAP bound on the relic abundance of LSP neutralino provides a stringent bound since the neutralino, in general, has a high relic abundance. On the other hand, even under such a strict constraint, it is possible to find solutions consistent with the WMAP bound by identifying some coannihilation channels which reduce the relic abundance of neutralino. Note that the solutions that are not consistent with the WMAP bound can still provide viable scenarios in conjunction with other form(s) of dark matter. As shown, for instance in Refs. [32,33], one can consider a Peccei-Quinn augmented MSSM [34] with NLSP neutralino and nonthermally produced axino as the LSP. The solutions in which the neutralino cannot saturate the dark matter are still viable in such a scenario.

In addition to these constraints, we require our solutions to be at least as consistent with the $(g-2)_\mu$ data as the standard model.

The current LHC results, especially after the discovery of the Higgs boson of mass about 125 GeV, have brought up discussions about naturalness of the supersymmetric models. On the other hand, null results of sparticle searches such as gluino at the LHC have also pushed the lower mass limits to more than 1 TeV in minimal supersymmetric scenarios. Moreover, a Higgs mass around 125 GeV also requires utilizing large radiative corrections and it mostly constrains the stop sector such that large stop masses [$\mathcal{O}(few - 10)$ TeV], or relatively large mixing between the two stops is necessary [35].

In the MSSM, in order to quantify naturalness or fine-tuning, one considers the electroweak scalar potential minimization condition which relates M_Z^2 to the SUSY breaking parameters $m^2_{H_{u,d}}$ and the parameter μ^2. The main implication from the naturalness of the electroweak scale is that the parameter μ should be of the order of 100 GeV [36,37]. In our case, if we require $t-b-\tau$ YU, with $\text{sign}(\mu) > 0$ and same sign gauginos, the SUSY threshold corrections to the bottom Yukawa coupling require large values of μ and m_0 (see [9] and references therein). We still chose to revisit this model in light of Higgs mass around 125 GeV and YU because it is the only model we know which yields NLSP gluino as the only channel available to realize the observed relic density. Moreover, we also note that by relaxing $t-b-\tau$ YU to $b-\tau$ YU, the stop-neutralino coannihilation scenario is also available.

Despite the nonuniversal gaugino masses at M_{GUT}, the model based on the gauge group $SU(4)_c \times SU(2)_L \times SU(2)_R$ can still be classified as a relatively minimal supersymmetric extension of the standard model, since it breaks into MSSM at M_{GUT} in our study, and it only has the stop sector for the large radiative corrections to realize the 125 GeV Higgs boson.

III. RESULTS

A. NLSP gluino and NLSP stop from $b-\tau$ YU

We quantify $b-\tau$ YU via the $R_{b\tau}$ parameter defined as [5]

$$R_{b\tau} = \frac{\max(y_b, y_\tau)}{\min(y_b, y_\tau)}, \tag{9}$$

where y_b and y_τ are Yukawa couplings at the GUT scale. $R_{b\tau}$ close to unity denotes acceptable $b-\tau$ YU. In Fig. 1, we plot $R_{b\tau}$ versus the fundamental parameters given in Eq. (2). Grey points are consistent with REWSB and LSP neutralino. Aqua points satisfy the various mass bounds which include the Higgs boson, as well as B-physics

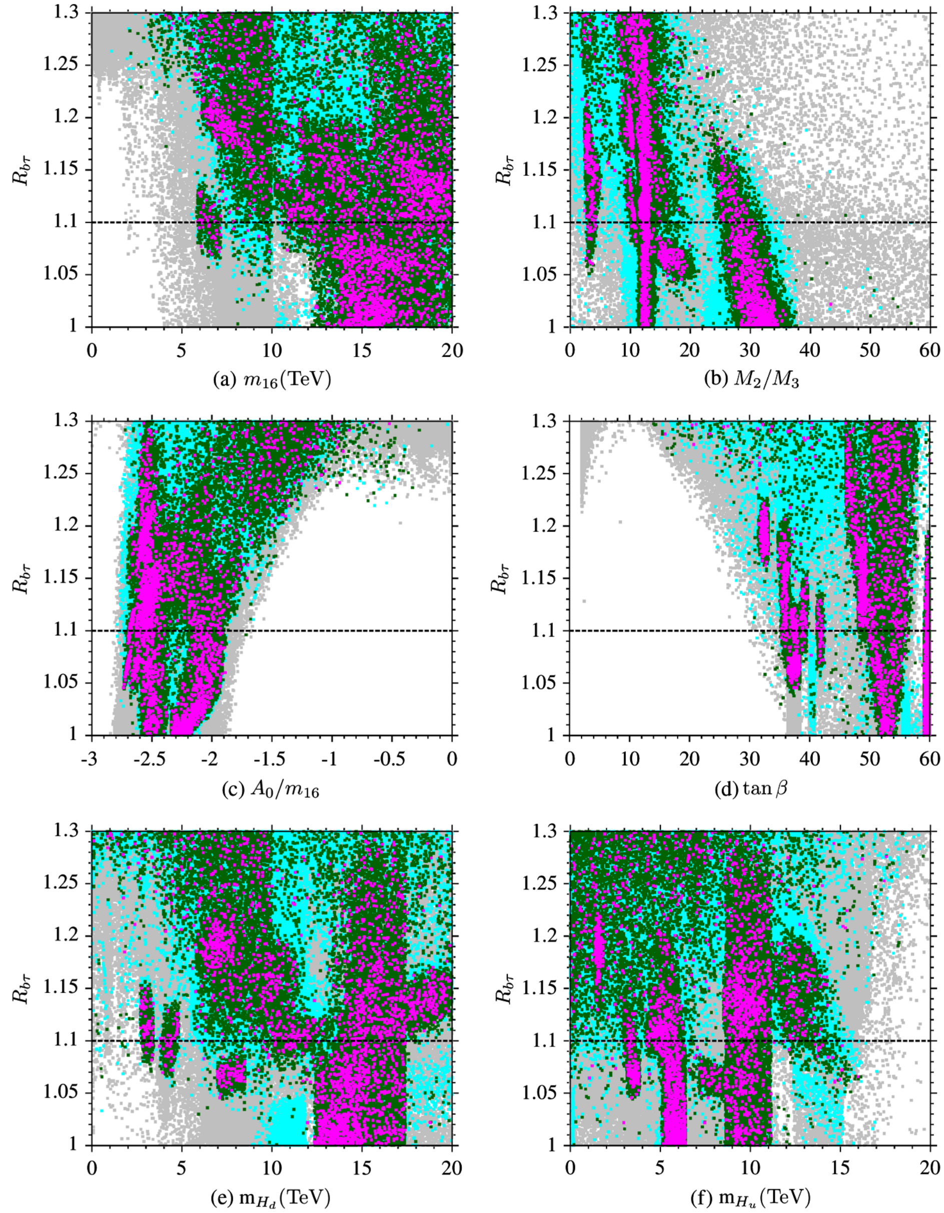

FIG. 1 (color online). (a–f) Plots in $R_{b\tau} - m_{16}$, $R_{b\tau} - M_2/M_3$, $R_{b\tau} - A_0/m_{16}$, $R_{b\tau} - \tan\beta$, $R_{b\tau} - m_{H_d}$, $R_{b\tau} - m_{H_u}$ planes. Grey points are consistent with REWSB and LSP neutralino. Aqua points satisfy mass bounds including bounds on Higgs mass and B-physics constraints. Green points belong to a subset of aqua and represent solutions with $\Omega h^2 \leq 1$. Magenta points form a subset of green points and satisfy the WMAP9 bound on relic abundance of LSP neutralino within 5σ.

constraints. Green points belong to a subset of aqua and represent solutions with $\Omega h^2 \leq 1$. Magenta points form a subset of green points and satisfy the WMAP9 bound within 5σ on the relic abundance of LSP neutralino.

In the $R_{b\tau} - m_{16}$ panel, we see that essentially perfect $b - \tau$ YU can be realized for $m_{16} \gtrsim 8$ TeV, while 10% or better $b - \tau$ YU requires $m_{16} \gtrsim 5$ TeV. We see from the $R_{b\tau} - M_2/M_3$ plot that we can have solutions with perfect $b - \tau$ YU for $M_2/M_3 \gtrsim 10$ in case of green or magenta points, while $b - \tau$ YU within 5%–10% is possible when $M_2/M_3 \sim 2$. The trilinear scalar coupling is found from the $R_{b\tau} - A_0/m_{16}$ panel to be in the range $-2.7 \lesssim A_0/m_{16} \lesssim -2.2$. The parameter $\tan\beta$ satisfies $30 \lesssim \tan\beta \lesssim 60$. The last two panels of Fig. 1 show the mass range of the MSSM Higgs fields.

Figure 2 displays plots in $m_{\tilde{g}} - m_{\tilde{\chi}_1^0}$, $\Delta m_{\tilde{g},\tilde{\chi}_1^0} - m_{\tilde{g}}$, $m_{\tilde{t}_1} - m_{\tilde{\chi}_1^0}$, $\Delta m_{\tilde{t}_1,\tilde{\chi}_1^0} - m_{\tilde{t}}$ planes, where $\Delta m_{\tilde{g},\tilde{\chi}_1^0} = m_{\tilde{g}} - m_{\tilde{\chi}_1^0}$ and $\Delta m_{\tilde{t}_1,\tilde{\chi}_1^0} = m_{\tilde{t}_1} - m_{\tilde{\chi}_1^0}$. Grey points are consistent with REWSB and LSP neutralino. Aqua points satisfy various mass bounds including bounds on the Higgs

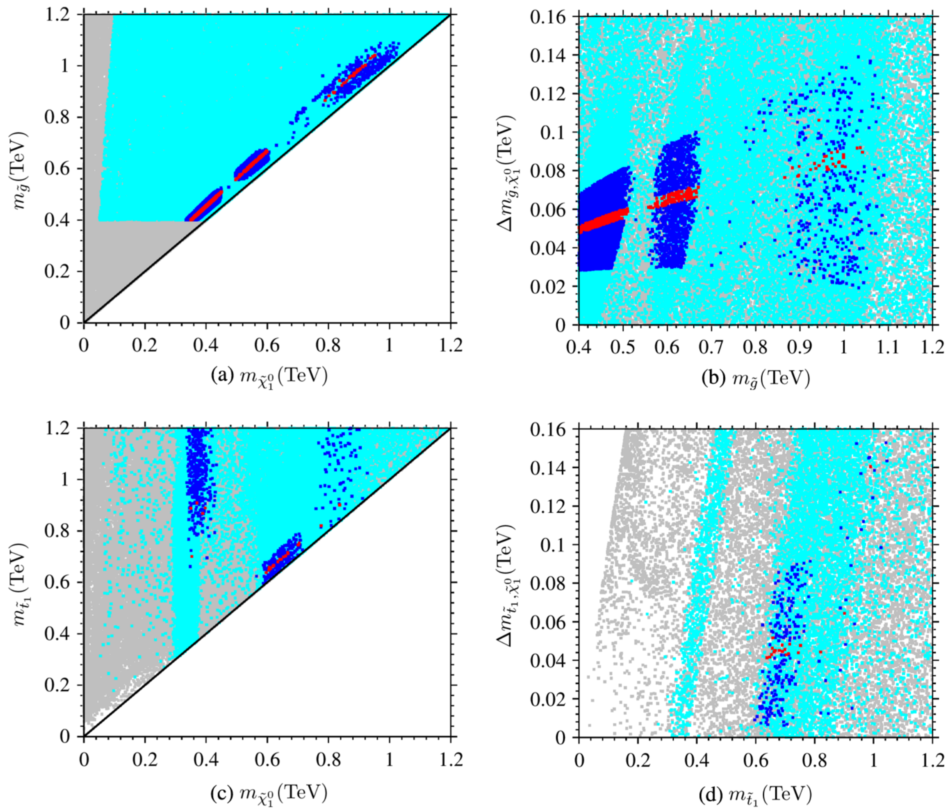

FIG. 2 (color online). (a–d) Plots in $m_{\tilde{g}} - m_{\tilde{\chi}_1^0}$, $\Delta m_{\tilde{g},\tilde{\chi}_1^0} - m_{\tilde{g}}$, $m_{\tilde{t}_1} - m_{\tilde{\chi}_1^0}$, $\Delta m_{\tilde{t}_1,\tilde{\chi}_1^0} - m_{\tilde{t}}$ planes where $\Delta m_{\tilde{g},\tilde{\chi}_1^0} = m_{\tilde{g}} - m_{\tilde{\chi}_1^0}$ and $\Delta m_{\tilde{t}_1,\tilde{\chi}_1^0} = m_{\tilde{t}_1} - m_{\tilde{\chi}_1^0}$. Grey points are consistent with REWSB and LSP neutralino. Aqua points satisfy mass bounds including bounds on Higgs mass and B-physics constraints. Blue points belong to a subset of aqua points and represent solutions with $\Omega h^2 \leq 1$ and $R_{b\tau} \leq 1.1$. Red points form a subset and they are consistent with the WMAP9 bound within 5σ.

mass and B-physics constraints. Blue points belong to a subset of aqua points and represent solutions with $\Omega h^2 \leq 1$ and $R_{b\tau} \leq 1.1$. Red points form a subset and they are consistent with the WMAP9 bound within 5σ. Let us discuss these graphs in some detail. In $t-b-\tau$ and $b-\tau$ YU, the third generation squarks are relatively light compared to those of the first two families. As a consequence, the gluino decay may lead to top-rich or bottom-rich decay signals. In the coannihilation region where $\Delta m_{\tilde{g},\tilde{\chi}_1^0} \ll 2m_t$, there is no phase space for on-shell top quarks. The gluino in this case decays into b jets, $\tilde{g} \to b\bar{b}\tilde{\chi}_1^0$, which enables one to search for the NLSP gluino via multi-b jets, namely

$$pp \to \tilde{g}\tilde{g} \to b\bar{b}b\bar{b} + \not{E}_T. \tag{10}$$

Such a scenario is favored for $\Delta m_{\tilde{g},\tilde{\chi}_1^0} \lesssim 100$ GeV. Note that the previous studies have ruled out a NLSP gluino with mass below 300 GeV [38].

We see from the top panels of Fig. 2 that the results for NLSP gluino with $b-\tau$ YU are similar to those obtained in the case of $t-b-\tau$ YU (as shown in the next section). For a NLSP gluino mass of the order of a TeV or so the mass difference with the LSP dark matter neutralino should be at least 50 GeV in order to be consistent with the WMAP9 bound (within 5σ) on dark matter relic abundance. In the region where the NLSP gluino is almost degenerate with the LSP neutralino ($\Delta m_{\tilde{g},\tilde{\chi}_1^0} \simeq 0$), the relic abundance of the latter is heavily reduced through coannihilation, thus making it inconsistent with the WMAP9 bound. It can be seen that our results with $m_{\tilde{g}} \gtrsim 800$ GeV avoid the exclusion limits reported in [39,40]. In Ref. [41], authors have considered gluino pair production at the 14 TeV LHC with subsequent decay of $\tilde{g}$ into light quarks and $\tilde{\chi}_1^0$. They have focused on $2/3/4$ jets $+ \not{E}_T$ signatures. From Fig. 2 of [41], we see that with an integrated luminosity of 30 fb^{-1}, NLSP gluino mass $m_{\tilde{g}} \gtrsim 857$ GeV and $m_{\tilde{g}} \gtrsim$ 1050 GeV can be excluded for $\Delta m_{\tilde{g},\tilde{\chi}_1^0} = 20$ GeV and $\Delta m_{\tilde{g},\tilde{\chi}_1^0} = 200$ GeV respectively. With an integrated luminosity of 100 fb^{-1}, the NLSP gluino mass exclusion limits rise up to $m_{\tilde{g}} \gtrsim 1000$ GeV for $\Delta m_{\tilde{g},\tilde{\chi}_1^0} = 20$ GeV, while $m_{\tilde{g}} \gtrsim 1275$ GeV for $\Delta m_{\tilde{g},\tilde{\chi}_1^0} = 200$ GeV can be tested at the LHC. Similar analysis can also be found in [42–44]. These studies show that our results can be probed at the LHC. It is indicated in [45] that in certain scenarios an LSP with mass $\gtrsim$600 GeV may evade the current LHC SUSY searches.

The bottom panels indicate a distinct property of $b-\tau$ YU in $4-2-2$ not found in $t-b-\tau$ YU. We found the NLSP stop solution in the $b-\tau$ case, with masses for the latter of order ~600–900 GeV. Note that NLSP stop solutions were previously found in the study of $b-\tau$ YU in SUSY $SU(5)$ in the mass range of ~100–400 GeV with $\tan\beta \gtrsim 20$ [32]. Our results are in agreement with the results previously reported in [46,47].

The bottom right panel shows that the mass difference between the NLSP stop and LSP neutralino should be at least 40 GeV to satisfy the WMAP9 dark matter abundance bound within 5σ. The search for NLSP stop in such a scenario is challenging and has been implemented both at the LEP and Tevatron [48–50]. The two-body stop decay into a top quark and neutralino or a bottom quark and chargino, and the three-body decay channels $\tilde{t}_1 \to W^+ b\tilde{\chi}_1^0$, $\tilde{t}_1 \to bl^+\tilde{\nu}$ are kinematically not allowed. The loop induced two-body decay of NLSP stop, $\tilde{t}_1 \to c\chi_1^0$, is generally considered to overwhelm the four-body channel $\tilde{t}_1 \to l^+\nu(q\bar{q}')b\tilde{\chi}_1^0$ and tends to be the dominant NLSP stop decay mode [51,52]. Results from searches for this decay channel using the Tevatron data have been reported by both the CDF and D0 experiments [53,54]. Both model independent and model dependent studies of stop-neutralino coannihilation show that regions of the parameter space with stop-neutralino mass difference of 20% are ruled out for $m_{\tilde{t}_1} \lesssim 140$ GeV [55,56]. Also, the first LHC searches for stop decaying into a charm quark and neutralino have recently been performed by the ATLAS collaboration [13] and stop masses up to 270 GeV have been excluded for LSP neutralino mass of about 200 GeV. On the other hand, $m_{\tilde{t}_1} = 250$ GeV with $\Delta m_{\tilde{t}_1,\tilde{\chi}_1^0} \leq 10$ GeV has been ruled out by a recent CMS analysis [14]. It is also shown that $m_{\tilde{t}_1} = 150$ GeV can be excluded for $m_{\tilde{\chi}_1^0} = 80$ GeV in two situations, (i) if $BR(\tilde{t}_1 \to c\tilde{\chi}_1^0) \leq 0.12$ and $BR(\tilde{t}_1 \to \tilde{\chi}_1^0 bf\bar{f}') \geq 0.88$ and (ii) if $BR(\tilde{t}_1 \to c\tilde{\chi}_1^0) \geq 0.43$ and $BR(\tilde{t}_1 \to \tilde{\chi}_1^0 bf\bar{f}') \leq 0.57$ [57].

The NLSP stop mass obtained from our analysis lies well beyond these exclusion limits, but we hope that the future LHC searches will probe it. We also find regions in the parameter space in which the stop and gluino masses are almost degenerate.

B. NLSP gluino from $t-b-\tau$ YU

In this section, we revisit $t-b-\tau$ YU in $4-2-2$ to update the results taking account of the current experimental constraints, and then compare with the results obtained for $b-\tau$ YU. We quantify $t-b-\tau$ YU with $R_{tb\tau}$ defined in the same way as was done for $b-\tau$ YU:

$$R_{tb\tau} = \frac{\max(y_t, y_b, y_\tau)}{\min(y_t, y_b, y_\tau)}. \tag{11}$$

We summarize our results for NLSP gluino in Fig. 3. The data displayed in this figure are generated separately from the one used in the previous section on $b-\tau$ YU. Color coding is the same as in Fig. 2, except that the condition $R_{b\tau} \leq 1.1$ is replaced with $R_{tb\tau} \leq 1.1$. The left panel shows that NLSP gluino with $m_{\tilde{g}} \gtrsim 1$ TeV can be realized consistent with $R_{tb\tau} \leq 1.1$ and all the experimental constraints. The NLSP gluino solutions consistent with 10% or better $t-b-\tau$ YU possess more or less the same features as previously discussed for $b-\tau$ YU.

Finally we present five benchmark points in Table I highlighting phenomenologically interesting features of the Yukawa unified $4-2-2$ model. All of these benchmark points satisfy the various constraints mentioned in Sec. II and are compatible with Yukawa unification. Points 1–4 are the examples of 10% or better $b-\tau$ YU. Points 1–2 display NLSP gluino solutions with $BF(\tilde{g} \to b\bar{b}\chi_1^0) \approx 0.58$. Point 3 represents an example where gluino is NLSP with $BF(\tilde{g} \to g\chi_1^0) \approx 0.83$ and stop is NNLSP while point 4 depicts the opposite example with $BF(\tilde{t}_1 \to c\chi_1^0) \approx 1.00$. Point 5 is an example of $t-b-\tau$ YU and exhibits a relatively heavy NLSP gluino solution with $R_{tb\tau} \approx 1.09$ and $BF(\tilde{g} \to b\bar{b}\chi_1^0) \approx 0.77$.

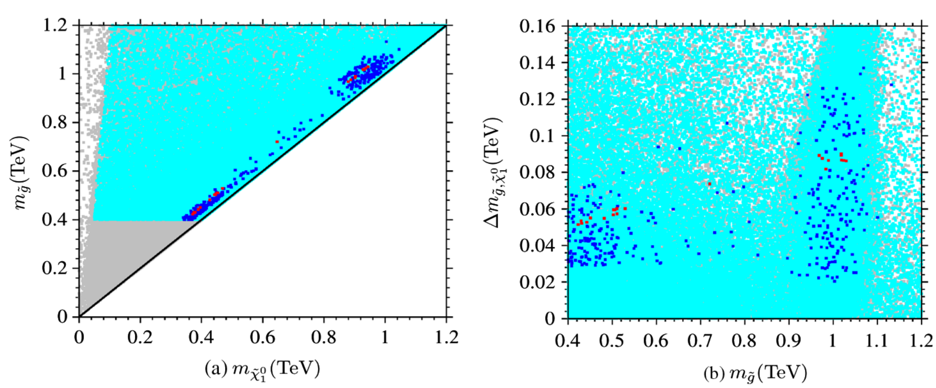

FIG. 3 (color online). (a,b) Plots in $m_{\tilde{g}} - m_{\tilde{\chi}_1^0}$ and $m_{\tilde{g},\tilde{\chi}_1^0}$ planes. Color coding is the same as in Fig. 2, except the $R_{b\tau} \leq 1.1$ condition is replaced with $R_{tb\tau} \leq 1.1$.

TABLE I. Sparticle and Higgs masses (in GeV units). Fundamental parameters are specified at $M_{\rm GUT}$. All of these benchmark points satisfy the various constraints mentioned in Sec. II and are compatible with Yukawa unification. Points 1–4 are examples of 10% or better $b-\tau$ YU. Points 1–2 display NLSP gluino solutions. Point 3 represents an example where gluino is NLSP and stop is NNLSP with a small mass difference while point 4 depicts the opposite example. Point 5 exhibits a relatively heavy NLSP gluino solution with $R_{tb\tau} = 1.09$.

	Point 1	Point 2	Point 3	Point 4	Point 5
m_{16}	19280	19460	11670	11940	19090
M_1	1864.96	1762.92	1729.84	1700	1795
M_2	2945	2790	2711	2660	2844
M_3	244.9	222.3	258.1	260.1	221.4
A_0/m_{16}	−2.691	−2.685	−2.631	−2.632	−2.52
$\tan\beta$	37.8	37.7	38.9	39	50.7
m_{H_d}	10890	11820	3246	3111	15640
m_{H_u}	4931	4555	5175	5478	9938
m_h	124	125	124	123	126
m_H	11254	12176	3357	3058	3253
m_A	11181	12097	3336	3039	3232
$m_{H^\pm}$	11255	12177	3359	3061	3255
$m_{\tilde{\chi}^0_{1,2}}$	952, 2794	903, 2659	850, 2481	837, 2441	928, 2728
$m_{\tilde{\chi}^0_{3,4}}$	22197, 22197	22407, 22407	12855, 12855	13101, 13101	19151, 19151
$m_{\tilde{\chi}^\pm_{1,2}}$	2891, 22246	2674, 22453	2497, 12844	2457, 13090	2735, 19151
$m_{\tilde{g}}$	1041	988	933	943	1018
$m_{\tilde{u}_{L,R}}$	19347, 19216	19520, 19374	11757, 11702	12019, 11977	19174, 18989
$m_{\tilde{t}_{1,2}}$	3107, 8349	3426, 8509	991, 5176	901, 5263	5692, 7556
$m_{\tilde{d}_{L,R}}$	19347, 19334	19520, 19522	11758, 11666	12019, 11933	19174, 19174
$m_{\tilde{b}_{1,2}}$	8405, 11088	8560, 11227	5205, 6881	5293, 7047	7414, 19098
$m_{\tilde{\nu}_1}$	19332	19487	11824	12091	19104
$m_{\tilde{\nu}_3}$	15837	15962	9848	10076	14208
$m_{\tilde{e}_{L,R}}$	19319, 19394	19474, 19600	11815	12081, 11906	19098, 19267
$m_{\tilde{\tau}_{1,2}}$	11668, 15838	11841, 15968	11645	7367, 10045	6806, 14137
σ_{SI}(pb)	2.49×10^{-14}	2.73×10^{-14}	7.44×10^{-15}	2.77×10^{-14}	1.67×10^{-14}
σ_{SD}(pb)	2.52×10^{-14}	2.82×10^{-14}	1.1×10^{-16}	6.09×10^{-17}	8.5×10^{-15}
$\Omega_{CDM}h^2$	0.116	0.102	0.112	0.122	0.124
$R_{b\tau}$, $R_{tb\tau}$	1.09	1.09	1.09	1.09	1.09

IV. CONCLUSION

We have explored $b-\tau$ and $t-b-\tau$ YU in supersymmetric $SU(4)_c \times SU(2)_L \times SU(2)_R$ $(4-2-2)$ models with the MSSM parameter $\mu > 0$. Our results extend earlier discussions of $4-2-2$ models and can be tested at LHC 14. We show that NLSP gluino masses of order 1 TeV are compatible with $b-\tau$ or $t-b-\tau$ Yukawa unification, while NLSP gluino masses of order 300 GeV or lower have now been excluded. We also display solutions in $b-\tau$ Yukawa unified models with NLSP stop masses $m_{\tilde{t}_1} \gtrsim 600$ GeV. In such cases, the mass difference between NLSP stop and LSP neutralino allows only the decays $\tilde{t}_1 \to c\tilde{\chi}^0_1$. This type of decay has recently been studied by the ATLAS and CMS collaborations, and our conclusions are consistent with their results. We also identify an interesting region of parameter space where NLSP and NNLSP masses are almost degenerate. In this region either the stop or gluino is the NLSP. We also revisit the supersymmetric $4-2-2$ model with $t-b-\tau$ YU which yields neutralino-gluino coannihilation solutions. This is the only channel compatible with the observed dark matter relic abundance. We find that NLSP gluino solutions in such a case have the same features as NSLP gluino in the $b-\tau$ YU scenario. We present five benchmark points as representatives of our solutions that may be tested in future LHC experiments.

ACKNOWLEDGMENTS

We thank Bin He, Jinmian Li, Tianjun Li and Jacob Wacker for useful discussions. This work is supported by the DOE Award No. DE-FG02-91ER40626 (S. R. and Q. S). This work used the Extreme Science and Engineering Discovery Environment (XSEDE), which is supported by the National Science Foundation Grant No. OCI-1053575.

[1] G. Aad *et al.* (ATLAS Collaboration), Phys. Lett. B **716**, 1 (2012).

[2] S. Chatrchyan *et al.* (CMS Collaboration), Phys. Lett. B **716**, 30 (2012); J. High Energy Phys. 06 (2013) 081.

[3] B. Ananthanarayan, G. Lazarides, and Q. Shafi, Phys. Rev. D **44**, 1613 (1991); Phys. Lett. B **300**, 245 (1993); Q. Shafi and B. Ananthanarayan, in *Proceedings of High energy physics and cosmology, Trieste, 1991*, p. 233, http://inspirehep.net/record/322651; J. C. Pati and A. Salam, Phys. Rev. D **10**, 275 (1974).

[4] See incomplete list of references, L. J. Hall, R. Rattazzi, and U. Sarid, Phys. Rev. D **50**, 7048 (1994); B. Ananthanarayan, Q. Shafi, and X. Wang, Phys. Rev. D **50**, 5980 (1994); R. Rattazzi and U. Sarid, Phys. Rev. D **53**, 1553 (1996); T. Blazek, M. Carena, S. Raby, and C. Wagner, Phys. Rev. D **56**, 6919 (1997); J. L. Chkareuli and I. G. Gogoladze, Phys. Rev. D **58**, 055011 (1998); T. Blazek, S. Raby, and K. Tobe, Phys. Rev. D **62**, 055001 (2000); H. Baer, M. Brhlik, M. Diaz, J. Ferrandis, P. Mercadante, P. Quintana, and X. Tata, Phys. Rev. D **63**, 015007 (2000); C. Balazs and R. Dermisek, J. High Energy Phys. 06 (2003) 024; U. Chattopadhyay, A. Corsetti, and P. Nath, Phys. Rev. D **66**, 035003 (2002); T. Blazek, R. Dermisek, and S. Raby, Phys. Rev. Lett. **88**, 111804 (2002); M. Gomez, T. Ibrahim, P. Nath, and S. Skadhauge, Phys. Rev. D **72**, 095008 (2005); K. Tobe and J. D. Wells, Nucl. Phys. **B663**, 123 (2003); I. Gogoladze, Y. Mimura, and S. Nandi, Phys. Lett. B **562**, 307 (2003); W. Altmannshofer, D. Guadagnoli, S. Raby, and D. M. Straub, Phys. Lett. B **668**, 385 (2008); S. Antusch and M. Spinrath, Phys. Rev. D **78**, 075020 (2008); H. Baer, S. Kraml, and S. Sekmen, J. High Energy Phys. 09 (2009) 005; S. Antusch and M. Spinrath, Phys. Rev. D **79**, 095004 (2009); K. Choi, D. Guadagnoli, S. H. Im, and C. B. Park, J. High Energy Phys. 10 (2010) 025; M. Badziak, M. Olechowski, and S. Pokorski, J. High Energy Phys. 08 (2011) 147; S. Antusch, L. Calibbi, V. Maurer, M. Monaco, and M. Spinrath, Phys. Rev. D **85**, 035025 (2012); J. S. Gainer, R. Huo, and C. E. M. Wagner, J. High Energy Phys. 03 (2012) 097; H. Baer, S. Raza, and Q. Shafi, Phys. Lett. B **712**, 250 (2012); M. Badziak, Mod. Phys. Lett. **27A**, 1230020 (2012); G. Elor, L. J. Hall, D. Pinner, and J. T. Ruderman, J. High Energy Phys. 10 (2012) 111; I. Gogoladze, Q. Shafi, and C. S. Un, Phys. Lett. B **704**, 201 (2011); J. High Energy Phys. 08 (2012) 028; M. A. Ajaib, I. Gogoladze, and Q. Shafi, Phys. Rev. D **88**, 095019 (2013); M. A. Ajaib, I. Gogoladze, Q. Shafi, and C. S. Un, J. High Energy Phys. 07 (2013) 139; arXiv:1308.4652.

[5] H. Baer, S. Kraml, S. Sekmen, and H. Summy, J. High Energy Phys. 03 (2008) 056; H. Baer, M. Haider, S. Kraml, S. Sekmen, and H. Summy, J. Cosmol. Astropart. Phys. 02 (2009) 002.

[6] I. Gogoladze, R. Khalid, and Q. Shafi, Phys. Rev. D **79**, 115004 (2009).

[7] H. Baer, S. Kraml, A. Lessa, and S. Sekmen, J. High Energy Phys. 02 (2010) 055.

[8] I. Gogoladze, R. Khalid, and Q. Shafi, Phys. Rev. D **80**, 095016 (2009).

[9] I. Gogoladze, R. Khalid, S. Raza, and Q. Shafi, J. High Energy Phys. 12 (2010) 055; I. Gogoladze, Q. Shafi, and C. S. Un, J. High Energy Phys. 07 (2012) 055.

[10] S. Profumo and C. E. Yaguna, Phys. Rev. D **69**, 115009 (2004); D. Feldman, Z. Liu, and P. Nath, Phys. Rev. D **80**, 015007 (2009); N. Chen, D. Feldman, Z. Liu, P. Nath, and G. Peim, Phys. Rev. D **83**, 035005 (2011).

[11] M. A. Ajaib, T. Li, Q. Shafi, and K. Wang, J. High Energy Phys. 01 (2011) 028.

[12] S. Antusch, S. F. King, and M. Spinrath, Phys. Rev. D **89**, 055027 (2014); S. Antusch and M. Spinrath, Phys. Rev. D **79**, 095004 (2009); S. Trine, S. Westhoff, and S. Wiesenfeldt, J. High Energy Phys. 08 (2009) 002 and references therein.

[13] G. Aad *et al.* (ATLAS Collaboration), Phys. Rev. D **90**, 052008 (2014).

[14] CMS Collaboration, Search for top squarks decaying to a charm quark and a neutralino in events with a jet and missing transverse momentum, Report No. CMS-PAS-SUS-13-009.

[15] R. Aaij *et al.* (LHCb Collaboration), Phys. Rev. Lett. **110**, 021801 (2013).

[16] G. Buchalla, A. J. Buras, and M. E. Lautenbacher, Rev. Mod. Phys. **68**, 1125 (1996).

[17] S. R. Choudhury and N. Gaur, Phys. Lett. B **451**, 86 (1999); K. S. Babu and C. F. Kolda, Phys. Rev. Lett. **84**, 228 (2000).

[18] H. Baer, F. E. Paige, S. D. Protopopescu, and X. Tata, arXiv:hep-th/0001086.

[19] J. Hisano, H. Murayama, and T. Yanagida, Nucl. Phys. **B402**, 46 (1993); Y. Yamada, Z. Phys. C **60**, 83 (1993); J. L. Chkareuli and I. G. Gogoladze, Phys. Rev. D **58**, 055011 (1998).

[20] D. M. Pierce, J. A. Bagger, K. T. Matchev, and R.-j. Zhang, Nucl. Phys. **B491**, 3 (1997).

[21] L. E. Ibanez and G. G. Ross, Phys. Lett. **110B**, 215 (1982); K. Inoue, A. Kakuto, H. Komatsu, and S. Takeshita, Prog. Theor. Phys. **68**, 927 (1982); K. Inoue, A. Kakuto, H. Komatsu, and S. Takeshita, Prog. Theor. Phys. **70**, 330 (1983); L. E. Ibanez, Phys. Lett. **118B**, 73 (1982); J. R. Ellis, D. V. Nanopoulos, and K. Tamvakis, Phys. Lett. **121B**, 123 (1983); L. Alvarez-Gaume, J. Polchinski, and M. B. Wise, Nucl. Phys. **B221**, 495 (1983).

[22] K. A. Olive *et al.* (Particle Data Group Collaboration), Chin. Phys. C **38**, 090001 (2014).

[23] Tevatron Electroweak Working Group and CDF Collaboration and D0 Collaboration, Report No. FERMILAB-TM-2427-E.

[24] I. Gogoladze, R. Khalid, S. Raza, and Q. Shafi, J. High Energy Phys. 06 (2011) 117.

[25] G. Belanger, F. Boudjema, A. Pukhov, and R. K. Singh, J. High Energy Phys. 11 (2009) 026; H. Baer, S. Kraml, S. Sekmen, and H. Summy, J. High Energy Phys. 03 (2008) 056.

[26] H. Baer and M. Brhlik, Phys. Rev. D **55**, 4463 (1997); H. Baer, M. Brhlik, D. Castano, and X. Tata, Phys. Rev. D **58**, 015007 (1998).

[27] K. Babu and C. Kolda, Phys. Rev. Lett. **84**, 228 (2000); A. Dedes, H. Dreiner, and U. Nierste, Phys. Rev. Lett. **87**, 251804 (2001); J. K. Mizukoshi, X. Tata, and Y. Wang, Phys. Rev. D **66**, 115003 (2002).

[28] D. Eriksson, F. Mahmoudi, and O. Stal, J. High Energy Phys. 11 (2008) 035.

[29] Y. Amhis *et al.* (Heavy Flavor Averaging Group Collaboration), arXiv:1207.1158.

[30] D. Asner *et al.* (Heavy Flavor Averaging Group Collaboration), arXiv:1010.1589.

[31] G. Hinshaw *et al.* (WMAP Collaboration), Astrophys. J. Suppl. Ser. **208**, 19 (2013).

[32] H. Baer, I. Gogoladze, A. Mustafayev, S. Raza, and Q. Shafi, J. High Energy Phys. 03 (2012) 047.

[33] T. Li, D. V. Nanopoulos, S. Raza, and X. C. Wang, J. High Energy Phys. 08 (2014) 128.

[34] R. Peccei and H. Quinn, Phys. Rev. Lett. **38**, 1440 (1977); R. Peccei and H. Quinn, Phys. Rev. D **16**, 1791 (1977); S. Weinberg, Phys. Rev. Lett. **40**, 223 (1978); F. Wilczek, Phys. Rev. Lett. **40**, 279 (1978); H. P. Nilles and S. Raby, Nucl. Phys. **B198**, 102 (1982); J. E. Kim, Phys. Lett. **136B**, 378 (1984); J. E. Kim and H. P. Nilles, Phys. Lett. **138B**, 150 (1984); for a review, see e.g. F. D. Steffen, Eur. Phys. J. C **59**, 557 (2009).

[35] M. Carena, S. Gori, N. R. Shah, and C. E. M. Wagner, J. High Energy Phys. 03 (2012) 014.

[36] H. Baer, V. Barger, D. Mickelson, and M. Padeffke-Kirkland, Phys. Rev. D **89**, 115019 (2014).

[37] R. Barbieri and G. F. Giudice, Nucl. Phys. **B306**, 63 (1988).

[38] M. A. Ajaib, T. Li, and Q. Shafi, Phys. Lett. B **705**, 87 (2011).

[39] ATLAS Collaboration, Search for strong production of supersymmetric particles in final states with missing transverse momentum and at least three b jets using 20.1 f^{-1} of pp collisions at $\sqrt{s} = 8$ TeV with the ATLAS detector, Report No. ATLAS-CONF-2013-061.

[40] CMS Collaboration, Phys. Lett. B **725**, 243 (2013).

[41] B. Bhattacherjee, A. Choudhury, K. Ghosh, and S. Poddar, Phys. Rev. D **89**, 037702 (2014).

[42] K. Harigaya, K. Kaneta, and S. Matsumoto, Phys. Rev. D **89**, 115021 (2014).

[43] S. Mukhopadhyay, M. M. Nojiri, and T. T. Yanagida, J. High Energy Phys. 10 (2014) 12.

[44] T. Cohen, T. Golling, M. Hance, A. Henrichs, K. Howe, J. Loyal, S. Padhi, and J. G. Wacker, J. High Energy Phys. 04 (2014) 117.

[45] T. Cheng, J. Li, and T. Li, J. Phys. G **42**, 065004 (2015).

[46] I. Gogoladze, S. Raza, and Q. Shafi, Phys. Lett. B **706**, 345 (2012).

[47] J. Ellis, K. A. Olive, and J. Zheng, Eur. Phys. J. C **74**, 2947 (2014).

[48] K. Nakamura *et al.* (Particle Data Group), J. Phys. G **37**, 075021 (2010).

[49] R. Demina, J. D. Lykken, K. T. Matchev, and A. Nomerotski, Phys. Rev. D **62**, 035011 (2000).

[50] CDF Collaboration, Report No. 9834, http://www.cdf.fnal.gov/physics/exotic/r2a/20090709.stop-charm/.

[51] K. I. Hikasa and M. Kobayashi, Phys. Rev. D **36**, 724 (1987); M. Muhlleitner and E. Popenda, J. High Energy Phys. 04 (2011) 095.

[52] A. D. Box and X. Tata, Phys. Rev. D **79**, 035004 (2009); **82**, 119905 (2010).

[53] T. Aaltonen *et al.* (CDF Collaboration), J. High Energy Phys. 10 (2012) 158.

[54] V. M. Abazov *et al.* (D0 Collaboration), Phys. Lett. B **665**, 1 (2008).

[55] M. A. Ajaib, T. Li, and Q. Shafi, Phys. Rev. D **85**, 055021 (2012).

[56] B. He, T. Li, and Q. Shafi, J. High Energy Phys. 05 (2012) 148.

[57] R. Grober, M. Muhlleitner, E. Popenda, and A. Wlotzka, arXiv:1408.4662.